

## ORIGINAL RESEARCH

# Abnormal splicing in the N-terminal variable region of cardiac troponin T impairs systolic function of the heart with preserved Frank-Starling compensation

Han-Zhong Feng<sup>1</sup>, Guozhen Chen<sup>2</sup>, Changlong Nan<sup>2</sup>, Xupei Huang<sup>2</sup> & Jian-Ping Jin<sup>1</sup><sup>1</sup> Department of Physiology, Wayne State University School of Medicine, Detroit, Michigan<sup>2</sup> Charles E. Schmidt College of Medicine, Florida Atlantic University, Boca Raton, Florida**Keywords**

Abnormal splicing, cardiac function, muscle contraction, N-terminal variable region, troponin T isoforms.

**Correspondence**

Jian-Ping Jin, Department of Physiology, Wayne State University School of Medicine, 540 E. Canfield, Detroit, MI 48201.  
Tel: 313-577-1520  
Fax: 313-577-5494  
E-mail: jjin@med.wayne.edu

**Funding Information**

This work was supported in part by grants from the National Institutes of Health (HL098945 and AR048816 to JPJ and HL112130 to XPH).

Received: 11 July 2014; Revised: 3 August 2014; Accepted: 6 August 2014

doi: 10.14814/phy2.12139

*Physiol Rep*, 2 (9), 2014, e12139,  
doi: 10.14814/phy2.12139

**Abstract**

Abnormal splice-out of the exon 7-encoded segment in the N-terminal variable region of cardiac troponin T (cTnT- $\Delta$ E7) was found in turkeys and, together with the inclusion of embryonic exon (eTnT), in adult dogs with a correlation with dilated cardiomyopathy. Overexpression of these cTnT variants in transgenic mouse hearts significantly decreased cardiac function. To further investigate the functional effect of cTnT- $\Delta$ E7 or  $\Delta$ E7+eTnT in vivo under systemic regulation, echocardiography was carried out in single and double-transgenic mice. No atrial enlargement, ventricular hypertrophy or dilation was detected in the hearts of 2-month-old cTnT- $\Delta$ E7 and  $\Delta$ E7+eTnT mice in comparison to wild-type controls, indicating a compensated state. However, left ventricular fractional shortening and ejection fraction were decreased in  $\Delta$ E7 and  $\Delta$ E7+eTnT mice, and the response to isoproterenol was lower in  $\Delta$ E7+eTnT mice. Left ventricular outflow tract velocity and gradient were decreased in the transgenic mouse hearts, indicating decreased systolic function. Ex vivo working heart function showed that high afterload or low preload resulted in more severe decreases in the systolic function and energetic efficiency of cTnT- $\Delta$ E7 and  $\Delta$ E7+eTnT hearts. On the other hand, increases in preload demonstrated preserved Frank-Starling responses and minimized the loss of cardiac function and efficiency. The data demonstrate that the N-terminal variable region of cardiac TnT regulates systolic function of the heart.

**Introduction**

The contraction and relaxation of skeletal and cardiac muscles are regulated by intracellular  $\text{Ca}^{2+}$  via troponin in the sarcomeric thin filament (Gordon et al. 2000). The troponin complex consists of three protein subunits, troponin C (TnC), troponin I (TnI) and troponin T (TnT). Troponin T coordinates the structure and function of troponin complex and is the thin filament anchoring molecule (Perry 1998). The N-terminal segment of TnT is a hypervariable region that differs among muscle type-specific isoforms and regulated via

alternative RNA splicing during development and adaptation (Wang and Jin 1998; Jin and Root 2000; Jin et al. 2000; Biesiadecki and Jin 2002; Biesiadecki et al. 2002, 2007; Feng et al. 2008).

Functional differences have been found between TnT isoforms and splice forms differing in the N-terminal variable region. A larger to smaller, more acidic to less acidic, switch occurs in the expression of both cardiac and fast skeletal muscle TnT during perinatal development (Cooper and Ordahl 1985; Jin and Lin 1989; Jin et al. 1992, 1996; Wang and Jin 1997). Biochemical and contractility studies have demonstrated functional

differences between embryonic and adult cardiac TnT (Jin and Lin 1989; Gomes et al. 2004).

Aberrant splicing of exon 4 that encodes 4–5 amino acids in the N-terminal variable region of cardiac TnT has been found in failing human hearts (Anderson et al. 1995; Mesnard-Rouiller et al. 1997), diabetic rat hearts (Akella et al. 1995), and hypertrophic rat hearts (McConnell et al. 1998). Abnormal omission of exon 8 occurs in turkey hearts with inherited dilated cardiomyopathy (Biesiadecki and Jin 2002). The same exon (exon 7 in mammalian cardiac TnT) was abnormally spliced out in dog hearts with dilated cardiomyopathy (cTnT- $\Delta$ E7) (Biesiadecki et al. 2002). This N-terminal region coding exon is constitutively included in normal cardiac TnT (Jin et al. 2008). Its aberrant splice-out in dilated turkey and dog cardiomyopathies indicates a causal relationship to the pathogenesis. In addition to the splice-out of exon 7, dilated cardiomyopathy dog hearts showed abnormal inclusion of the embryonic exon 5 in cardiac TnT (eTnT) in the adult cardiac muscle (Biesiadecki et al. 2002).

The coexistence of two or more cTnT variants resulting in split myofilament  $Ca^{2+}$  sensitivity (Biesiadecki et al. 2002; Gomes et al. 2004) would cause a temporally desynchronized myofilament response to the rising of intracellular  $Ca^{2+}$  during the activation of contraction. After the alternative splicing-generated cTnT isoform switch during perinatal heart development (Jin and Lin 1988), a single form of cardiac troponin is present in adult cardiac muscle of human and most other vertebrates, corresponding to the notion that a uniformed  $Ca^{2+}$  activation of the thin filaments generates a synchronized contraction. Our previous studies have demonstrated that the coexistence of functionally distinct TnT isoforms (Huang et al. 1999) or N-terminal splicing variants (Huang et al. 2008; Feng and Jin 2010; Wei et al. 2010) with altered  $Ca^{2+}$  activation of force production resulted in decreased pumping function and energetic efficiency. Further evidence from chronic coexistence of two TnT isoforms in adult transgenic mouse heart also showed decreased contractile and  $Ca^{2+}$  transient kinetics in cardiomyocytes (Yu et al. 2012).

The present study investigated the pathogenic phenotype of the abnormally spliced variants cardiac TnT in vivo in transgenic mice overexpressing cTnT- $\Delta$ E7 or  $\Delta$ E7 + eTnT at young age prior to the development of anatomical cardiomyopathy using echocardiography under systemic neurohumoral regulation, followed by ex vivo working heart studies on isolated organ function. In addition to detecting early changes in cardiac function, the results showed that the N-terminal abnormality of cardiac TnT impaired systolic function and energetic efficiency, whereas Frank-Starling response of the heart was preserved to compensate cardiac function, providing valuable insights into the structure-function relationship of troponin and the pathogenic mechanism for cTnT N-terminal abnormality to generate dilated cardiomyopathy.

## Methods

### Ethical approval

All animal protocols are approved by the Institutional Animal Care and Use Committees of Wayne State University and Florida Atlantic University, and conformed to the guidelines of the National Institutes of Health Guide for the Care and Use of Laboratory Animals.

### Transgenic mice

The two transgenic mouse lines used in this study have been generated in previous studies to postnatally overexpress cTnT- $\Delta$ E7 or eTnT (Fig. 1) under the control of an  $\alpha$ -myosin heavy chain (MHC) promoter in C57BL/6 strain (Biesiadecki et al. 2002).

Double-transgenic mice were generated by crossing the cTnT- $\Delta$ E7 and eTnT lines to combine the overexpression of  $\Delta$ E7+eTnT. Genotyping of the transgenic mice was carried out using PCR on tail biopsies as described previously (Huang et al. 1999). We have previously demonstrated that the total level of myocardial TnT remained normal in the single and double-transgenic mouse lines

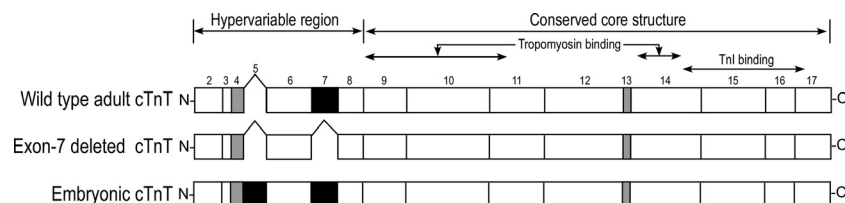


**Figure 1.** Abnormal splicing variants of cardiac TnT. The primary structural alignment shows the N-terminal splicing patterns of wild-type adult cardiac TnT, exon 7-deleted cardiac TnT and embryonic cardiac TnT. The developmentally regulated exon 5 and abnormally deleted exon 7 are shown as solid black boxes. Exons 4 and 13 that are also alternatively spliced in normal mouse cardiac TnT are shown as gray boxes. The tropomyosin- and TnI-binding sites (Jin and Chong 2010; Wei and Jin 2011) are outlined.

(Feng and Jin 2010), which provides effective replacement models for functional studies.

Mice were maintained on a 12:12-h light-dark cycle (6:00 AM/6:00 PM) and fed with standard pellet diet. Two-month-old female mice were used for echocardiographic measurement and 3- to 5-month-old mice of both sexes were used for ex vivo working heart studies.

### Echocardiography

Echocardiography studies were performed using a Vevo 770 high-resolution in vivo imaging system (VisualSonics, Toronto, ON, Canada) as described previously (Li *et al.* 2013). To exclude experimental bias, all measurements were done by an examiner blinded to the genotypes. The mice were anesthetized with 1.2% isoflurane and placed on a heating pad to maintain body temperature at 37°C. Hair on the precordial region was removed with Nair lotion hair remover, and the region was covered with ultrasound transmission gel (Aquasonic, Parker Laboratory, Fairfield, NJ). Short-axis images under the M-mode were taken to view the left ventricle (LV) and right ventricle (RV) movements during diastole and systole, allowing us to measure the ventricular structure and dimension. Transmitral blood flow was measured with Pulse Doppler and diastolic mitral annular velocity was measured with Tissue Doppler. After measurement of baseline condition, isoproterenol (ISO) was administered (0.2 mg kg<sup>-1</sup> body weight, i.p.) and the same measurement was repeated for  $\beta$ -adrenergic responses. All data and images were saved and analyzed with the Advanced Cardiovascular Package Software (VisualSonics) to evaluate cardiac function.

### Ex vivo working heart studies

Transgenic and wild-type mouse hearts were examined in isolated ex vivo working heart preparations as previously described (Feng *et al.* 2008). Thirty minutes after injection of 100 Unit heparin i.p., mice were anesthetized with pentobarbital (100 mg kg<sup>-1</sup> body weight, i.p.). Hearts were rapidly isolated and cannulated via aorta with a modified 18-gauge needle to start Langendorff retrograde perfusion within 3 min after opening of the chest. A pressure sensor (MLT844 pressure transducer, Capto, Horten, Norway) was connected to the side arm of aortic cannular and placed at the level equivalent to the heart to measure aortic pressure. A 0.5 mL air bubble was introduced in the aortic trap to mimic in vivo arterial compliance. A pulmonary vein was then cannulated with a 16-gauge needle for perfusion to the left atria in the working mode. The pulmonary artery trunk was connected to a beveled polyethylene-25 tubing to collect the coronary effluent from the right ventricle. The coronary effluent was also

measured for the O<sub>2</sub> concentration by passing through an O<sub>2</sub> sensor (Microelectrode). The apex was punctured using a 30-gauge needle to make a path that allows the insertion of a 1.2-Fr pressure-volume (P-V) catheter (Sci-sense, London, ON, Canada) into the LV. After all the cannulations were established, a water jacket was placed around the heart to maintain the surrounding temperature at 37°C before switching to left atrial perfusion to start the working mode.

The perfusion medium used was a modified Krebs-Henseleit bicarbonate buffer equilibrated with 95% O<sub>2</sub>-5% CO<sub>2</sub>, containing 118 m·mol·L<sup>-1</sup> NaCl, 4.7 m·mol·L<sup>-1</sup> KCl, 1.2 m·mol·L<sup>-1</sup> KH<sub>2</sub>PO<sub>4</sub>, 2.25 m·mol·L<sup>-1</sup> MgSO<sub>4</sub>, 2.25 m·mol·L<sup>-1</sup> CaCl<sub>2</sub>, 0.32 m·mol·L<sup>-1</sup> EGTA, 2 m·mol·L<sup>-1</sup> pyruvate, and 15 m·mol·L<sup>-1</sup> D-glucose. NaHCO<sub>3</sub> was added to adjust the pH to 7.4 at 37°C. The perfusion buffer was filtered with a 0.45- $\mu$ m filter membrane and not reused.

Baseline cardiac function was recorded at the standard preload of 10 mmHg and afterload of 55 mmHg (Barbato *et al.* 2005). Heart rate was controlled at 480 beats per min with supraventricular pacing using an isolated constant current stimulator (A365; World Precision Instruments, Sarasota, FL) through a pair of custom-modified platinum wires attached to the surface of right atrium.

Aortic and coronary effluent volumes were recorded in real time by calibrated counting of drops of the outflow. Pressure and volume development data were collected at a sampling rate of 1 kHz with 100-Hz filter using a Powerlab 16-channel analog-to-digital interface and Chart 5.0 software (AD Instruments, Colorado Springs, CO). Preload response was tested by altering the height of preload perfusate reservoir at left atrial filling pressure of 5, 8, 10, 12.5, 15, and 20 mmHg. Afterload was adjusted by changing the height of effluent outlet equivalent to 55, 70, or 90 mmHg.

Immediately after functional measurements, LV muscle tissue was collected from each heart and stored at -80°C for Western blot verification of cardiac TnT contents.

### Time parameters of ex vivo working heart function

Left ventricular ejection time parameters were determined as previously described (Feng and Jin 2010). Briefly, the opening and closing of the aortic valve were identified by analyzing the traces of aortic pressure (AP). The first and highest peak of +dP/dt of AP, indicating the full opening of the aortic valve, was used as the beginning of the ejection. The lowest point of the AP curve at the end of the ejection phase, at which the dP/dt of AP = 0, was used as the time of aortic valve closing. The duration between these two points is the total LV ejection time. The rapid ejection phase was from the beginning of ejection to the

peak of LV pressure (LVP). Isovolumetric contraction time was defined from the beginning of systole in LVP trace to the time of aortic valve opening. The isovolumetric relaxation time was measured from the end of ejection to the time when LVP decreased to the level of left atrial filling pressure that was equal to the preload.

### Calculation of cardiac efficiency

Cardiac efficiency was first evaluated by the ratio between LV ejection integral (the area under LVP curve during the ejection phase) and LV total integral (the total area under the LVP curve).

Left ventricular efficiency was further calculated from  $O_2$  consumption as previously described (Neely et al. 1967; Gauthier et al. 1998; Feng and Jin 2010): Cardiac efficiency (in %) = cardiac work/myocardial  $O_2$  consumption  $\times 100$ . Myocardial  $O_2$  consumption was calculated from the difference between  $O_2$  concentrations in the perfusion influent and coronary effluent:  $O_2$  consumption (in  $mL \cdot O_2 \cdot min^{-1} \cdot g^{-1}$ ) =  $(PO_{2a} - PO_{2v}) \times$  coronary flow  $\times c/760$  where  $PO_{2a}$  is  $PO_2$  in the perfusate (95%),  $PO_{2v}$  is  $PO_2$  in the coronary effluent, and  $c$  is the solubility coefficient for  $O_2$  in Krebs buffer ( $22.7 mL O_2 \cdot atm^{-1} \cdot mL^{-1}$  at  $37^\circ C$ ).

Pressure work and kinetic work were calculated as follows: Pressure work (in  $J \cdot min^{-1} \cdot g^{-1}$ ) = cardiac output (in  $mL \cdot min^{-1} \cdot g^{-1}$ )  $\times$  aortic pressure (in mmHg)  $\times 1.33 \times 10^{-4} J \cdot mmHg^{-1} \cdot mL^{-1}$ . Kinetic work (in  $J \cdot min^{-1} \cdot g^{-1}$ ) = cardiac output (in  $mL \cdot min^{-1} \cdot g^{-1}$ )  $\times$  [perfusate density (in  $g \cdot cm^{-3}$ )/ $980 \text{ cm}^3 \cdot s^{-2}$ ]  $\times V^2 \times 9.8 \times 10^{-3} J \cdot g^{-1} \cdot m^{-1} \cdot min^{-1} \cdot g^{-1}$  where  $V$  (in  $cm \cdot s^{-1}$ ) = [cardiac output (in  $mL \cdot min^{-1}$ )/aortic cross-sectional area (in  $cm^2$ )]  $\times$  [cycle time (in s)/ejection time (in s)]  $\times (1/60)$ . Myocardial  $O_2$  consumption was converted into joules per minute per gram using a conversion factor of  $20.054 J \cdot mL^{-1} O_2$  consumed (Gauthier et al. 1998).

### SDS-polyacrylamide gel electrophoresis (PAGE) and western blotting

Cardiac muscle from left ventricular free wall was rapidly isolated postmortem and homogenized in SDS-PAGE sample buffer containing 2% SDS and 1%  $\beta$ -mercaptoethanol, pH 8.8, using a high speed mechanical homogenizer to extract total proteins. The SDS-PAGE samples were denatured by heating at  $80^\circ C$  for 5 min, centrifuged in a microcentrifuge to remove insoluble materials, and resolved on 14% SDS-gel with an acrylamide:bisacrylamide ratio of 180:1 using a modified Laemmli buffer system in which both stacking and resolving gels were at pH 8.8. The protein bands resolved in the gel were stained with Coomassie Blue R-250. Total protein in each lane

was quantified by ImageJ software (National Institutes of Health, Bethesda, MD) for normalizing the amount of sample loading.

Duplicate SDS-gels were transferred to nitrocellulose membrane using a Bio-Rad semidry electrical transfer device at constant current of  $5 \text{ mA cm}^{-2}$  for 15 min. The blotted membranes were blocked in 1% bovine serum albumin (BSA) in Tris-buffered saline (TBS,  $150 \text{ m} \cdot \text{mol L}^{-1} \text{ NaCl}$ ,  $50 \text{ m} \cdot \text{mol L}^{-1} \text{ Tris}$ , pH 7.5) with shaking at room temperature for 30 min. The blocked membrane was probed with an anti-TnI monoclonal antibody (mAb) TnI-1 (Jin et al. 2001) or an anti-TnT mAb 2C8 that recognizes all TnT isoforms and splice forms (Jin and Chong 2010), both diluted in TBS containing 0.1% BSA, with gentle rocking at  $4^\circ C$  overnight. The membranes were then washed three times with TBS containing 0.5% Triton X-100 and 0.05% SDS for 7 min each time and following with two times wash of TBS for 3 min of each time. After incubation with alkaline phosphatase-labeled goat anti-mouse IgG second antibody (Santa Cruz Biotechnology, Dallas, TX) at room temperature for 1 hour, membranes were washed again as above, and developed in 5-bromo-4-chloro-3-indolyl phosphate/nitro blue tetrazolium substrate solution to visualize the cardiac TnI and cardiac TnT bands.

### Pro-Q diamond phosphoprotein staining

To examine the effect of  $\beta$ -adrenergic-dependent phosphorylation of thin and thick filament proteins, Pro-Q Diamond phosphoprotein staining (Invitrogen, Grand Island, NY) was employed following the manufacturer's instruction. Total cardiac muscle proteins were resolved on 14% SDS-polyacrylamide gels as above. The SDS-gel was fixed in 50% methanol and 10% acetic acid overnight with a change after the first 45 min. After washing in deionized water for three changes of 10 min each, the gel was stained with shaking in Pro-Q Diamond reagent for 90 min in a dark box. Destaining was performed in 20% acetonitrile,  $50 \text{ m} \cdot \text{mol} \cdot \text{L}^{-1}$  sodium acetate, pH 4.0, for three changes of 30 min each in a dark box. The gel was then washed twice with deionized water for 5 min each in a dark box and scanned on a Typhoon 9410 fluorescence scanner (GE Healthcare, Wauwatosa, WI) with excitation at 532 nm and recording the emission at 560 nm to reveal phosphorylated proteins. The same gel was then stained with Coomassie Blue R-250 to visualize the total protein profile.

### Data analysis

Data are presented as means  $\pm$  SE or  $\pm$  SD and statistical analysis was performed using Student's *t* test, or one-way

and two-way ANOVA with a Fisher adjustment as noted in the table and figure legends.

## Results

### Impaired systolic function of cTnT- $\Delta$ E7 and $\Delta$ E7+eTnT transgenic mouse hearts in vivo

B-mode and M-mode echocardiography showed no atrial or ventricular enlargement or dilation in the transgenic mice in comparison with the wild-type (WT) control at 2 months of age. Figure 2 shows representative images of the left ventricle under M-mode and aortic blood flow under pulse wave Doppler for the three groups. Consistently normalized left ventricular mass values indicated no significant LV hypertrophy in the transgenic mice (Table 1). The results indicate no cardiac remodeling at anatomical level in the young mouse hearts and reflect a compensated state of these cardiomyopathy models.

The results in Fig. 3A and B showed that LV fractional shortening (FS) and ejection fraction (EF), the most commonly used indexes of global LV systolic function, measured using echocardiography were both decreased in cTnT- $\Delta$ E7 and  $\Delta$ E7+eTnT transgenic mouse hearts as compared to WT control. Isoproterenol stimulation significantly increased FS and EF of WT and cTnT- $\Delta$ E7 hearts, whereas the response was minimum in  $\Delta$ E7+eTnT hearts (Fig. 3A and B). Whereas the beta-adrenergic response of pump function (FS and EF) was blunted, contractile velocity was unchanged  $\Delta$ E7+eTnT hearts (Table 1). While the molecular mechanism remains to be investigated, this phenotype is

consistent with the more severely decreased stroke volume (Fig. 9E) and cardiac efficiency (Fig. 10B) of the  $\Delta$ E7+eTnT hearts.

No significant change was found in mitral Doppler and tissue Doppler measurements (Table 1), except that left ventricular contraction time (LVCT) was increased in  $\Delta$ E7+eTnT mice as compared to that of WT and cTnT- $\Delta$ E7 mice, suggesting a lower LV contractile velocity in the  $\Delta$ E7+eTnT hearts. In contrast, left ventricular relaxation time (LVRT) did not show significant change in the transgenic mouse hearts.

To evaluate the kinetic function of the heart, left ventricular outflow tract (LVOT) velocity was measured from the apical approach in an anteriorly angulated four-chamber view. Aortic Doppler data indicated that LVOT velocity and LVOT gradient were decreased in cTnT- $\Delta$ E7 and  $\Delta$ E7+eTnT hearts as compared to WT control (Fig. 3C and D). LVOT velocity and gradient were both flow dependent. The results indicate less flow at aortic valves during systole resulting from reduced systolic function in cTnT- $\Delta$ E7 and  $\Delta$ E7+eTnT mouse hearts.  $\Delta$ E7+eTnT hearts showed less response of LVOT velocity and LVOT gradient to isoproterenol stimulation in comparison with that of WT and cTnT- $\Delta$ E7 hearts (Fig. 3C and D).

### No change in phosphorylation of cardiac TnI and myosin-binding protein C in vivo

Pro-Q diamond phosphoprotein staining of SDS-PAGE gels examined the phosphorylation level of cardiac TnI and myosin-binding protein C in mouse hearts under isoproterenol treatment in vivo (Fig. 4). The results did not find significant difference among the three groups,

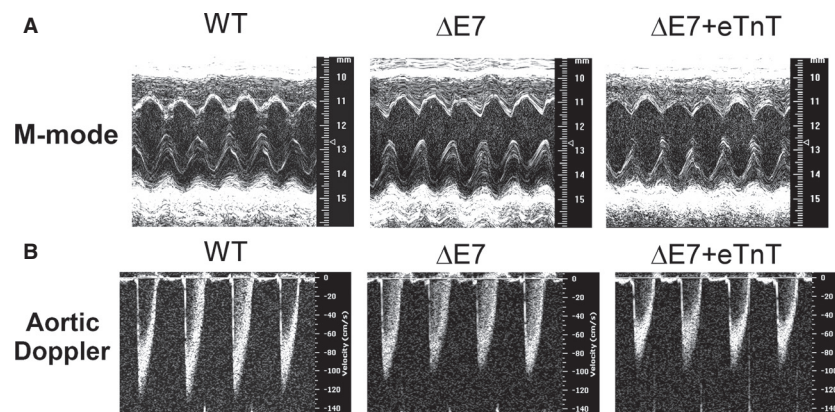


**Figure 2.** Decreased systolic function of transgenic mouse hearts detected in vivo using echocardiography. (A) M-mode echocardiography showed motion (M) of the interfaces toward and away from the transducer along with the time axis. The results indicated a larger left ventricular end systolic dimension and volume in cTnT- $\Delta$ E7 and  $\Delta$ E7+eTnT than that in WT mice. (B) Doppler spectrum of the aorta showed that the velocity of blood flow during ejection was slower in cTnT- $\Delta$ E7 and  $\Delta$ E7+eTnT mice than that of WT group.

**Table 1.** In vivo cardiac function measured with echocardiography.

Parameters	WT	$\Delta E7$	$\Delta E7+eTnT$
Body weight (g)	17.54 $\pm$ 0.36	17.31 $\pm$ 0.57	18.4 $\pm$ 0.61
Heart rate (bpm)	482 $\pm$ 4	483 $\pm$ 2	488 $\pm$ 4
LV end diastole			
IVS (mm)	0.82 $\pm$ 0.04	0.82 $\pm$ 0.03	0.81 $\pm$ 0.04
PW (mm)	0.74 $\pm$ 0.05	0.65 $\pm$ 0.06	0.63 $\pm$ 0.07
LVEDD (mm)	2.89 $\pm$ 0.11	3.07 $\pm$ 0.14	3.07 $\pm$ 0.07
LV Volume ( $\mu$ L)	32.18 $\pm$ 3.00	37.66 $\pm$ 4.07	37.28 $\pm$ 2.15
LV End Systole			
IVS (mm)	1.31 $\pm$ 0.04	1.26 $\pm$ 0.06	1.20 $\pm$ 0.09
PW (mm)	1.30 $\pm$ 0.06	1.14 $\pm$ 0.07	1.10 $\pm$ 0.10
LVESD (mm)	1.44 $\pm$ 0.06	1.74 $\pm$ 0.07*	1.72 $\pm$ 0.06*
LV Volume ( $\mu$ L)	5.61 $\pm$ 0.53	9.16 $\pm$ 0.92*	8.75 $\pm$ 0.70*
LV EF %	83.09 $\pm$ 1.08	75.44 $\pm$ 1.46*	76.21 $\pm$ 2.23*
LV FS %	50.51 $\pm$ 1.25	43.22 $\pm$ 1.27*	43.95 $\pm$ 2.30*
LV Mass Corrected, mg	53.57 $\pm$ 2.30	54.49 $\pm$ 2.41	53.03 $\pm$ 5.04
Mitral Pulsed Doppler			
E velocity ( $\text{mm}\cdot\text{s}^{-1}$ )	712.11 $\pm$ 5.82	704.24 $\pm$ 0.75	677.46 $\pm$ 7.79
A velocity ( $\text{mm}\cdot\text{s}^{-1}$ )	561.36 $\pm$ 17.46	456.36 $\pm$ 15.91	423.21 $\pm$ 23.95
E/A	1.27 $\pm$ 0.04	1.59 $\pm$ 0.11	1.63 $\pm$ 0.10
LVRT (ms)	16.27 $\pm$ 0.42	17.90 $\pm$ 1.20	17.70 $\pm$ 0.88
LVCT (ms)	9.20 $\pm$ 0.40	9.13 $\pm$ 0.50	11.02 $\pm$ 0.74* <sup>#</sup>
Mitral TDI			
E' velocity ( $\text{mm}\cdot\text{s}^{-1}$ )	30.44 $\pm$ 0.05	31.33 $\pm$ 0.80	29.31 $\pm$ 0.41
A' velocity ( $\text{mm}\cdot\text{s}^{-1}$ )	22.35 $\pm$ 0.25	23.40 $\pm$ 1.32	21.25 $\pm$ 0.37
E'/A'	1.37 $\pm$ 0.02	1.36 $\pm$ 0.05	1.40 $\pm$ 0.05
E/E'	23.39 $\pm$ 0.19	22.53 $\pm$ 0.53	23.12 $\pm$ 0.29
Aortic Pulsed Doppler			
Ao Peak Velocity ( $\text{mm}\cdot\text{s}^{-1}$ )	1242.40 $\pm$ 31.94	1040.70 $\pm$ 26.73*	1006.70 $\pm$ 76.22*
Ao Peak Gradient (mmHg)	6.20 $\pm$ 0.32	4.36 $\pm$ 0.22*	4.16 $\pm$ 0.33*
Ao Mean Gradient (mmHg)	1.79 $\pm$ 0.11	1.27 $\pm$ 0.08	1.21 $\pm$ 0.77
Ao Velocity Time Integral (cm)	4.15 $\pm$ 0.17	3.62 $\pm$ 0.20	3.34 $\pm$ 0.25*

Data are presented as mean  $\pm$  SE,  $n = 5$  mice in each group. \* $P < 0.05$  compared to WT and <sup>#</sup> $P < 0.05$  compared between cTnT- $\Delta E7$  and  $\Delta E7+eTnT$  groups using Student's *t* test.

suggesting that  $\beta$ -adrenergic signaling was preserved and the impaired systolic function may indicate direct effects of cTnT- $\Delta E7$  or  $\Delta E7+eTnT$  on cardiac muscle contractility. Representing other phosphorylation-regulated myofilament proteins, the phosphorylation level of myosin regulatory light chain (RLC) also had no significant change in the cTnT- $\Delta E7$  and  $\Delta E7+eTnT$  mouse hearts (Fig. 4C).

### cTnT- $\Delta E7$ and $\Delta E7+eTnT$ decreased systolic function of ex vivo working hearts

To exclude the effects of neurohumoral and vascular compensation on cardiac function in vivo, isolated ex vivo working heart preparations under precisely con-

trolled preload, afterload and heart rate provide further information for the effects of cTnT- $\Delta E7$  or  $\Delta E7+eTnT$  on the function of cardiac muscle. In addition to baseline measurements at preload of 10 mmHg and afterload of 55 mmHg, 70 mmHg, and 90 mmHg were used to apply afterload stress. The results showed that in WT hearts,  $\pm dP/dt$  and maximum LVP ( $LVP_{\max}$ ) increased at higher afterloads, whereas stroke volume decreased in response to the increase in afterload (Fig. 5).

cTnT- $\Delta E7$  and  $\Delta E7+eTnT$  hearts had significantly slower systolic and diastolic velocities (Fig. 5A and B),  $LVP_{\max}$  (Fig. 5C), and stroke volume (Fig. 5D) than that of WT hearts at baseline and more severe at higher afterloads. The diastolic LVP ( $LVP_{\min}$ ) was unchanged (data not shown), indicating that the end diastolic pressure and

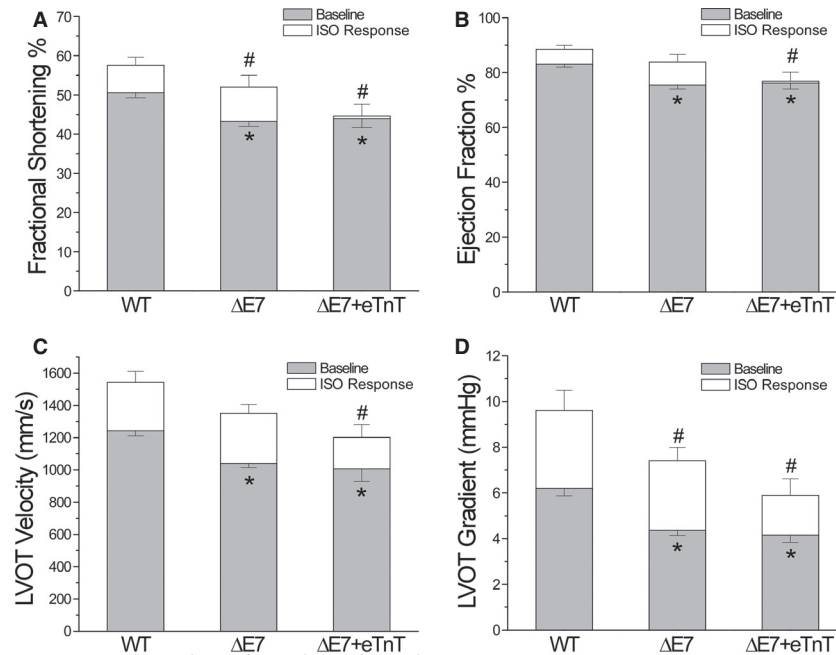


**Figure 3.** Effects of isoproterenol on cardiac function in vivo. (A and B) Baseline fraction shortening (FS) and ejection fraction (EF) were significantly decreased in cTnT-ΔE7 and ΔE7+eTnT mouse hearts as compared to WT controls. Upon isoproterenol (ISO) stimulation, FS and EF in WT and cTnT-ΔE7 mouse hearts were increased, whereas ΔE7+eTnT hearts had no significant response to ISO stimulation. (C and D) Aortic Doppler data demonstrated that left ventricular outflow track (LVOT) velocity and gradient were decreased significantly in cTnT-ΔE7 and ΔE7+eTnT mice compared to that of WT mice. ISO produced increases in all groups, whereas the levels remained lower in cTnT-ΔE7 and ΔE7+eTnT hearts than that of WT control. The values are mean ± SD.  $n = 5$  in each group. \* $P < 0.05$ , compared to WT at baseline and # $P < 0.05$ , compared to WT upon ISO treatment, in Student's  $t$  test.

myocardial compliance did not change in the transgenic mouse hearts under normal or increased afterloads. The inability to increase  $\pm dP/dt$  in cTnT-ΔE7 and ΔE7+eTnT hearts when afterload was increased suggests a diminished contractile capacity.

When afterload was increased, the time parameters of WT mouse hearts showed decreased total, rapid, and reduced ejection times (Fig. 6A), corresponding to the reduced stroke volume (Fig. 5D). Total ejection time was prolonged in cTnT-ΔE7 hearts and reduced ejection time was shortened in ΔE7+eTnT hearts. There were similar decreases in total and reduced ejection time of cTnT-ΔE7 and ΔE7+eTnT hearts when afterload was increased. At 90 mmHg rapid ejection time did not shorten significantly in cTnT-ΔE7 and ΔE7+eTnT hearts when afterload was increased, therefore, was longer than that of WT (Fig. 6A).

Isovolumetric contraction and relaxation times (IVCT and IVRT) were longer in cTnT-ΔE7 and ΔE7+eTnT hearts than WT controls at all afterloads tested (Fig. 6B), indicating slower initial systolic and diastolic velocities (Fig. 5A and B) in comparison to that of WT hearts.

### Decreased efficiency of cTnT-ΔE7 and ΔE7+eTnT hearts

LVP integral and ejection integral were increased when afterload was increased in all three groups of hearts, in which the ejection integral had proportionally less increase indicating decreased pumping efficiency under high afterload (Fig. 7A). An increase in ejection integral reflects increased stroke work during ejection, while the increase in LVP integral corresponds to increased energy consumption. The pumping efficiency calculated from LVP ejection integral versus total integral detected that ΔE7+eTnT hearts had lower efficiency at 55 and 70 mmHg afterloads as compared with WT controls (Fig. 7B).

To further investigate the decreased cardiac efficiency using the classic approach of measuring cardiac output versus oxygen consumption, the results showed that pressure work was lower in cTnT-ΔE7 and ΔE7+eTnT hearts than that in WT hearts at all afterloads tested (Fig. 8A). Pressure work was increased in WT but not cTnT-ΔE7 and ΔE7+eTnT hearts when afterload was increased (Fig. 8A). Kinetic work was decreased

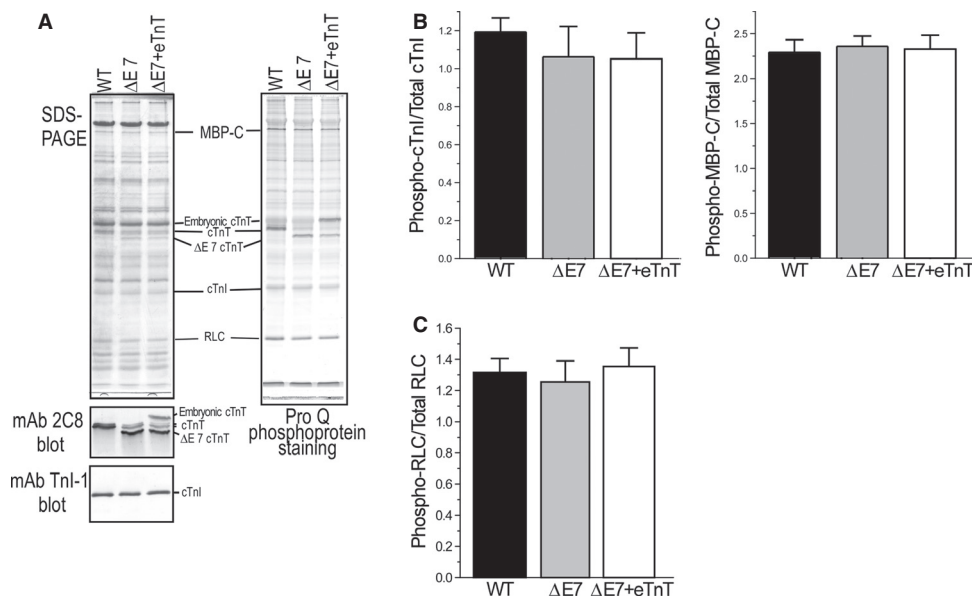


**Figure 4.**  $\beta$ -adrenergic-dependent phosphorylation of cardiac TnI and MBP-C was preserved. (A) Normalized to the level of actin, SDS-PAGE gel and Pro-Q staining showed no significant difference in the phosphorylation levels of cardiac TnI and MBP-C in WT, cTnT- $\Delta$ E7 and  $\Delta$ E7+eTnT mouse hearts in vivo under isoproterenol (ISO) stimulation. mAb 2C8 Western blot confirmed the expression of cTnT- $\Delta$ E7 and eTnT in the transgenic mouse hearts. mAb TnI-1 Western blot showed similar levels of cardiac TnI in all three groups. (B) Densitometry quantification showed no statistical difference among the three groups. (C) There was also no difference in the phosphorylation of myosin regulatory light chain among the three groups. The values are mean  $\pm$  SE.  $n = 5$  mice in each group. Statistical analysis was done using one-way ANOVA.

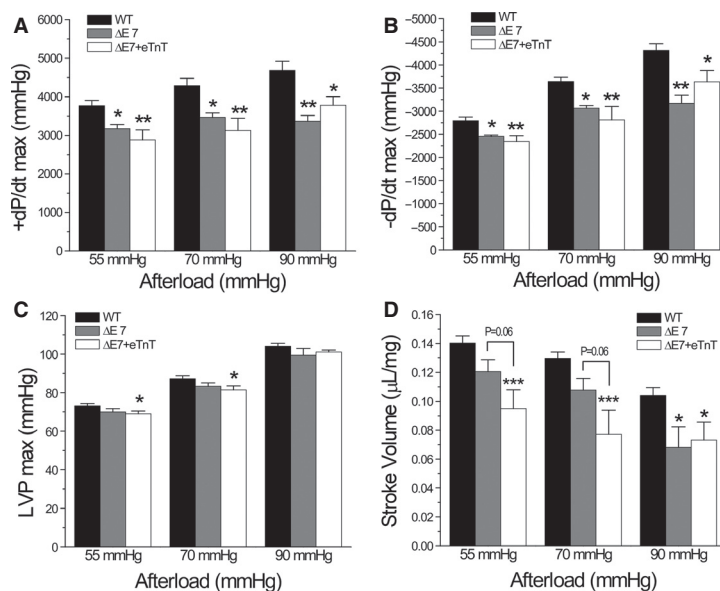


**Figure 5.** Working heart performance at different afterloads. (A and B)  $+dP/dt_{max}$  and  $-dP/dt_{max}$  were increased when afterload was increased from 55 mmHg to 90 mmHg in WT hearts.  $+dP/dt_{max}$  and  $-dP/dt_{max}$  were significantly slower in cTnT- $\Delta$ E7 and  $\Delta$ E7+eTnT hearts than WT controls with minimum responses to the increases in afterload. (C)  $LVP_{max}$  increased in all three groups in response to increases in afterload.  $\Delta$ E7+eTnT hearts produced lower  $LVP_{max}$  than that of WT hearts at 55 mmHg and 70 mmHg afterloads. (D) Stroke volume decreased in response to increases in afterload in all groups. cTnT- $\Delta$ E7, and more obviously  $\Delta$ E7+eTnT hearts, had significantly lower stroke volume than that of WT hearts at all afterloads tested.  $n = 10$  in WT,  $n = 5$  in cTnT- $\Delta$ E7 and  $n = 6$  in  $\Delta$ E7+eTnT groups. The values are mean  $\pm$  SE. \* $P < 0.05$  and \*\* $P < 0.01$  versus WT groups in one-way ANOVA.

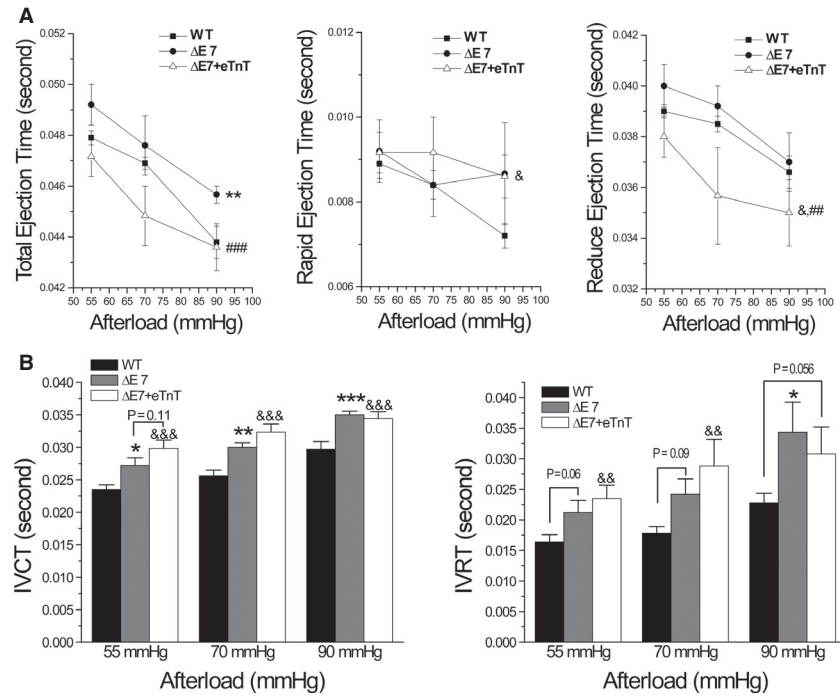


**Figure 6.** Time parameters of working heart at different afterloads. (A) Similar trends of decrease in total and reduced ejection time were seen in cTnT-ΔE7, ΔE7+eTnT and WT hearts when afterload was increased from 55 to 90 mmHg. Total and reduced ejection times were longer in cTnT-ΔE7 hearts but shorter in ΔE7+eTnT hearts as compared to that of WT hearts. Rapid ejection time was longer in cTnT-ΔE7 and ΔE7+eTnT hearts than WT control at 90 mmHg afterload. (B) Indicating slower initial systolic and diastolic velocities, IVCT, and IVRT increased in all three groups when afterload was increased and were longer in cTnT-ΔE7 and ΔE7+eTnT hearts than that of WT hearts.  $n = 10$  in WT,  $n = 5$  in cTnT-ΔE7 and  $n = 6$  in ΔE7+eTnT groups. The values are mean  $\pm$  SE. \* $P < 0.05$ , \*\* $P < 0.01$ , and \*\*\* $P < 0.001$  cTnT-ΔE7 versus WT; & $P < 0.05$  and && $P < 0.001$  ΔE7+eTnT versus WT; ## $P < 0.01$  and ### $P < 0.001$  ΔE7+eTnT versus cTnT-ΔE7. Statistical tests were performed using two-way ANOVA for panel A and one-way ANOVA for panel B.

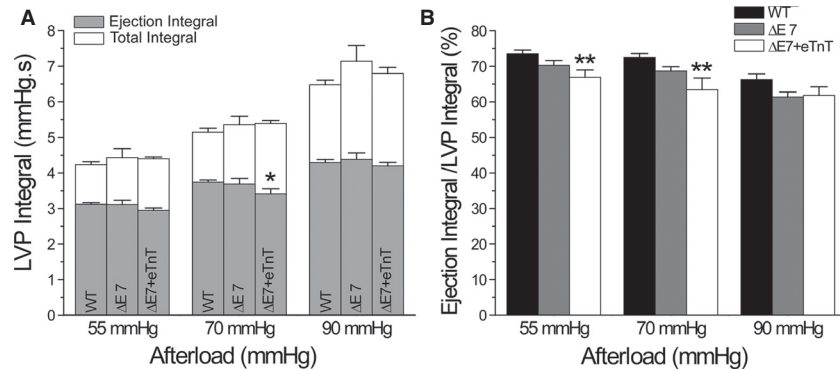


**Figure 7.** Cardiac efficiency indicated by LVP integrals. (A) Ejection integral was lower in ΔE7+eTnT hearts than that of WT hearts at 70 mmHg afterload. (B) The ratio of ejection integral versus total LVP integral was lower in ΔE7+eTnT hearts at 55 and 70 mmHg afterload than WT control.  $n = 10$  in WT,  $n = 5$  in cTnT-ΔE7 and  $n = 6$  in ΔE7+eTnT groups. The values are mean  $\pm$  SE. \* $P < 0.05$  and \*\* $P < 0.01$  versus WT in one-way ANOVA.

(Fig. 8A) and  $MVO_2$  increased in all three groups of hearts when afterload was increased. These changes resulted in a reduction of energetic efficiency that was more severe in cTnT-ΔE7 and ΔE7+eTnT hearts than

that in WT hearts and diminished more at higher afterload in all three groups (Fig. 8B). It was worth noting that although  $MVO_2$  was lower in cTnT-ΔE7 and ΔE7+eTnT hearts than that of WT hearts

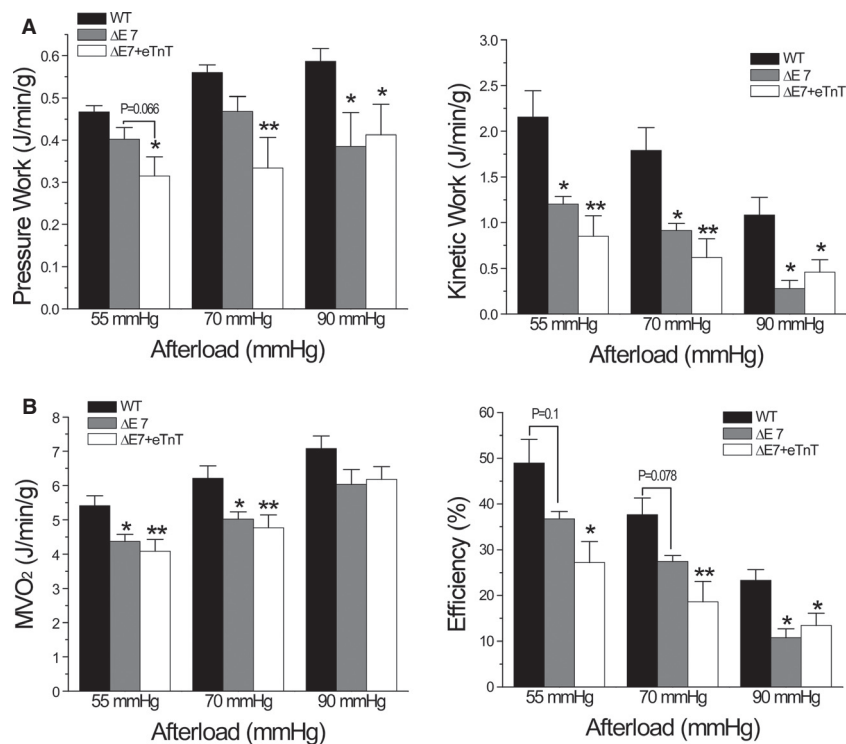


**Figure 8.** Cardiac efficiency determined from oxygen consumption. (A) WT hearts showed increased pressure work and decreased kinetic work when afterload was increased. cTnT-ΔE7 and ΔE7+eTnT hearts produced lower pressure work and kinetic work than that of WT hearts. Increases in afterload decreased kinetic work in cTnT-ΔE7 and ΔE7+eTnT hearts like that in WT hearts without significantly altering pressure work. (B) Oxygen consumption (MVO<sub>2</sub>) was increased in all three groups when afterload was increased, in which cTnT-ΔE7 and ΔE7+eTnT hearts showed lower values than WT control. Cardiac efficiency calculated from the external cardiac work (the sum of pressure work and kinetic work) versus MVO<sub>2</sub> was decreased in cTnT-ΔE7 and, more severely, in ΔE7+eTnT hearts. Increases in afterload decreased cardiac efficiency in all three groups and augmented the difference between cTnT-ΔE7 and ΔE7+eTnT hearts and WT control.  $n = 10$  in WT,  $n = 5$  in cTnT-ΔE7 and  $n = 6$  in ΔE7+eTnT groups. The values are mean  $\pm$  SE. \* $P < 0.05$  and \*\* $P < 0.01$  versus WT. in two-way ANOVA.

(Fig. 8B), the ratio of cardiac work versus energy expenditure was significantly lower in cTnT-ΔE7 and ΔE7+eTnT hearts due to drastically decreased work, corresponding to lower energetic efficiency (Fig. 8B).

### Preserved response to preload in cTnT-ΔE7 and ΔE7+eTnT hearts

At afterload of 55 mmHg and heart rate of 480 beats per minute, increases in preload enhanced ventricular function as measured by  $\pm$ dP/dt, LVP, and stroke volume (Fig. 9), similarly in WT, cTnT-ΔE7 and ΔE7+eTnT hearts. Although functions of cTnT-ΔE7 and ΔE7+eTnT hearts were consistently lower than WT controls at the wide range of preload tested (Fig. 9), the results demonstrated preserved Frank-Starling response in cTnT-ΔE7 and ΔE7+eTnT hearts, which were capable of compensating for the impaired systolic function.

In WT hearts, raising preload increased both ejection integral and LVP integral (data not shown) as a result

of increased contractility. Pumping efficiency deduced from the ratio of ejection integral to LVP integral increased when preload increased from 5 mmHg to 10 mmHg whereas further increases in preload did not produce significant change (Fig. 10A). cTnT-ΔE7 and ΔE7+eTnT hearts had lower pumping efficiency, which was improved when preload was increased, reaching the level of WT control at 20 mmHg (Fig. 10A).

The effect of increasing preload on improving energetic efficiency of cTnT-ΔE7 and ΔE7+eTnT hearts was further demonstrated by the ratio of cardiac work versus oxygen consumption (Fig. 10B). Cardiac efficiency was significantly lower in cTnT-ΔE7 and ΔE7+eTnT hearts than that of WT hearts at all preloads tested (Fig. 10B). Therefore, impaired systolic function appeared to be a determining factor in reducing myocardial energetic efficiency. However, increases in preload did improve energetic efficiency of cTnT-ΔE7 and ΔE7+eTnT hearts (Fig. 10B). The results confirmed the effect of increasing preload on

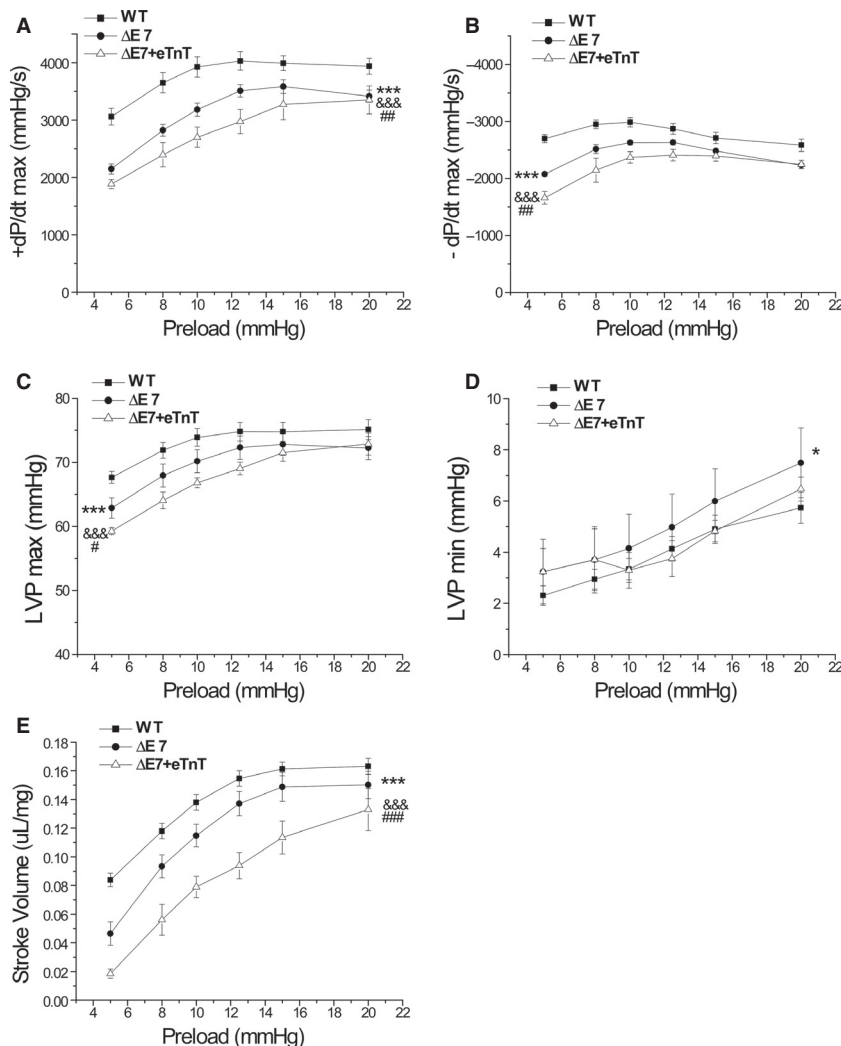


**Figure 9.** Response of ex vivo working hearts to changes in preload. (A and B) Systolic (+dP/dt<sub>max</sub>) and diastolic (-dP/dt<sub>max</sub>) velocities of cTnT- $\Delta E7$  and  $\Delta E7+eTnT$  hearts were significantly slower than that of WT hearts at all preloads tested. Comparing to cTnT- $\Delta E7$ ,  $\Delta E7+eTnT$  hearts had slower  $\pm dP/dt_{max}$  at preloads from 5 to 12.5 mmHg. (C) LVP<sub>max</sub> was lower in cTnT- $\Delta E7$  than that of WT hearts.  $\Delta E7+eTnT$  hearts showed further decreases in LVP<sub>max</sub> at preloads of 5 to 12.5 mmHg. (D) LVP<sub>min</sub> increased in all three groups when preload was increased. cTnT- $\Delta E7$  hearts had higher LVP<sub>min</sub> than that of WT hearts. (E) Stroke volume increased when preload was increased and reached to a plateau at 15 mmHg in WT and cTnT- $\Delta E7$  hearts. Stroke volume of cTnT- $\Delta E7$  hearts was significantly lower than that of WT hearts at all preloads tested.  $\Delta E7+eTnT$  hearts had further decreased stroke volume at all preloads tested but it continued the increase at 20 mmHg preload.  $n = 10$  in WT,  $n = 5$  in cTnT- $\Delta E7$  and  $n = 6$  in  $\Delta E7+eTnT$  groups. Values are mean  $\pm$  SE. \* $P < 0.05$  and \*\*\* $P < 0.001$  cTnT- $\Delta E7$  versus WT; &&& $P < 0.001$   $\Delta E7+eTnT$  versus WT; ## $P < 0.01$  and ### $P < 0.001$   $\Delta E7+eTnT$  versus cTnT- $\Delta E7$ , in two-way ANOVA.

compensating for the impaired systolic function of cTnT- $\Delta E7$  and  $\Delta E7+eTnT$  hearts.

## Discussion

cTnT- $\Delta E7$  is an aberrant splicing variant found in turkey and dog dilated cardiomyopathies (Biesiadecki and Jin 2002; Biesiadecki et al. 2002). The embryonic splice form of cardiac TnT normally expresses in embryonic

and neonatal heart and skeletal muscle (Jin 1996). Its expression in adult heart is found coexisting with cTnT- $\Delta E7$  in dogs with dilated cardiomyopathy (Biesiadecki et al. 2002) as represented by the  $\Delta E7+eTnT$  double-transgenic mice. Extended from previous studies, the present work demonstrated the pathophysiology of cTnT- $\Delta E7$  and  $\Delta E7+eTnT$  in transgenic mouse models in vivo and ex vivo with the following new findings.

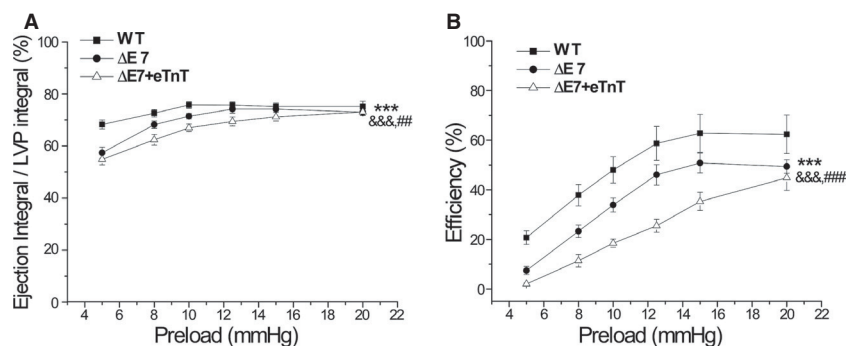


**Figure 10.** Cardiac efficiency in responses to preload. (A) Pumping efficiency calculated as the ratio of ejection integral versus LVP integral was increased when preload was increased from 5 to 10 mmHg in WT hearts. cTnT-ΔE7 and ΔE7+eTnT hearts had lower pumping efficiency than that of WT hearts at preloads of 5 to 12.5 mmHg, which was increased to reach the WT level at high preload of 20 mmHg. (B) Cardiac efficiency calculated as the ratio of cardiac work to  $\text{MVO}_2$  was significantly lower in cTnT-ΔE7 and ΔE7+eTnT hearts than that of WT hearts. Increases in preload increased the efficiencies of cTnT-ΔE7 and ΔE7+eTnT hearts, which, however, remained lower than WT control.  $n = 10$  in WT,  $n = 5$  in ΔE7 and  $n = 6$  in ΔE7+eTnT groups. Values are mean  $\pm$  SE.  $***P < 0.001$  cTnT-ΔE7 versus WT;  $***P < 0.001$  ΔE7+eTnT versus WT;  $##P < 0.01$  and  $###P < 0.001$  ΔE7+eTnT versus cTnT-ΔE7 in two-way ANOVA.

### Effects of cardiac TnT N-terminal abnormality on systolic function of the heart

Quantitative studies on multiple functional parameters demonstrated that cTnT-ΔE7 and cTnT-ΔE7+eTnT hearts had specifically decreased systolic function both in vivo and in ex vivo working heart preparations. cTnT-ΔE7 and eTnT differ from wild-type adult cardiac TnT in the N-terminal region (Biesiadecki et al. 2002). The N-terminal region of TnT is a variable structure that differs among muscle type-specific isoforms and is regulated by alternative splicing during heart and muscle development and adaptation (Wei and Jin 2011). In previous studies, we and others have demonstrated the function of the N-terminal variable region in regulating myofilament  $\text{Ca}^{2+}$  sensitivity (Biesiadecki and Jin 2002; Gomes et al. 2004; Mamidi et al. 2013a) and interaction with tropomyosin. An overall observation is that a longer N-terminal segment with more negatively charged residues produces higher  $\text{Ca}^{2+}$  sensitivity (Reiser et al. 1992, 1996; Ogut et al. 1999; Mamidi et al. 2013b).

Consistent with the nature of the N-terminal segment of TnT as a regulatory structure, N-terminal abnormal splicing has been detected in failing human hearts (Anderson et al. 1995; Mesnard-Rouiller et al. 1997). Another example for the regulatory function of the N-terminal segment of cardiac TnT is its selective removal by restrictive proteolysis in adaptation to ischemia-reperfusion or pressure overload (Zhang et al. 2006; Feng et al. 2008). Overexpression of the N-terminal truncated cTnT resulted in decreased contractile velocity in transgenic mice (Feng et al. 2008), supporting the notion that

modification in the N-terminal region of cardiac TnT regulates systolic function of the heart.

### Impaired systolic function and TnT heterogeneity decrease cardiac efficiency

The ventricular ejection time is a crucial parameter in determining cardiac output and energetic efficiency (Braunwald et al. 1958; Sarnoff et al. 1958; Weissler et al. 1968; Lewis et al. 1977; Geeraerts et al. 2004; Gutterman and Cowley 2006; Feng and Jin 2010). The N-terminal variation of cardiac TnT plays a role on regulating the time of ventricular ejection. For example, N-terminal truncated cardiac TnT prolongs the rapid ejection phase by moderately reducing systolic velocity without decreasing  $\text{LVP}_{\text{max}}$ , which increases cardiac efficiency (Feng et al. 2008). Similarly, Fig. 6A showed that cTnT-ΔE7 and ΔE7+eTnT hearts had prolonged rapid ejection phase, especially at higher afterload (90 mm Hg).

However, the compensatory effect of prolonged ejection time of cTnT-ΔE7 and ΔE7+eTnT hearts did not completely correct the decreased cardiac efficiency due to their effects on decreasing  $\text{LVP}_{\text{max}}$  that severely reduced systolic function. In addition, ΔE7+eTnT hearts had even shorter total and reduced ejection times than that of WT hearts, reflecting worse systolic function. We previously demonstrated that TnT heterogeneity, i.e., the coexistence of more than one class of TnT in the cardiac myofilaments, decreased heart function and energetic efficiency by desynchronizing myofilaments' response to the rising and decaying of cytosolic  $\text{Ca}^{2+}$  (Huang et al. 2008; Yu et al. 2012). IVCT and IVRT that reflect nonwork energy

consumption were prolonged in cTnT- $\Delta$ E7 and more in  $\Delta$ E7+eTnT hearts (Fig. 6B) due to decreased systolic and diastolic velocities, consistent with desynchronized myofilament actions and decreased energetic efficiency from increasing nonwork energy consumption. These dominantly negative effects could explain the decreased efficiency in cTnT- $\Delta$ E7 hearts and more obviously in  $\Delta$ E7+eTnT hearts.

The mechanisms by which the N-terminal variable region of cardiac TnT affects  $\text{Ca}^{2+}$  sensitivity and systolic function of the heart require further study. Results from this line of investigation may identify a therapeutic range of decreasing myofilament  $\text{Ca}^{2+}$  sensitivity to prolong rapid ejection time without significant decrease in force development and  $\text{LVP}_{\text{max}}$ .

### Preserved Frank-Starling response partially compensate for the impaired systolic function of cTnT- $\Delta$ E7 and $\Delta$ E7+eTnT hearts

Indicated by the similar left ventricular end diastolic dimension seen in echocardiographs (Table 1) and  $\text{LVP}_{\text{min}}$  in response of afterloads (data not shown), the young cTnT- $\Delta$ E7 and  $\Delta$ E7+eTnT transgenic mouse hearts were at a compensated stage without anatomical dilation or clinical failure.

The results in Fig. 9 showed preserved Frank-Starling response of cTnT- $\Delta$ E7 and  $\Delta$ E7+eTnT hearts, demonstrating that the N-terminal abnormality in cardiac TnT does not abolish the Frank-Starling regulation of cardiac muscle. Diastolic function of the ventricular muscle is one of the key factors that determine the Frank-Starling response of the heart, which may be separated from the negative effect of cardiac TnT N-terminal abnormality on systolic function.

Nonetheless, a chronic adaptive utilization of Frank-Starling mechanism to compensate for the impaired systolic function would increase energy expenditure and induce dilatative ventricular remodeling, leading to the progression of dilated cardiomyopathy in cTnT- $\Delta$ E7 and  $\Delta$ E7+eTnT hearts (Yu et al. 2012).

### Potential benefit when eTnT is expressed together with cTnT- $\Delta$ E7

While cTnT- $\Delta$ E7 is an abnormally spliced mutant form of cardiac TnT, eTnT is a normal TnT naturally expressed in embryonic hearts (Jin and Lin 1989). cTnT- $\Delta$ E7 was found in both turkey and dog dilated cardiomyopathies as a primary pathogenic abnormality. While the dominantly negative impact and pathogenic effects of exon 7 deletion in cardiac TnT have been demonstrated (Wei et al. 2010), the effect of the expression of embryonic

cardiac TnT in adult heart on the development of dilated cardiomyopathy is worth investigating.

The contractility data in Fig. 5A showed that while cTnT- $\Delta$ E7 hearts failed to have positive inotropic responses when afterload increased from 70 mmHg to 90 mmHg,  $\Delta$ E7+eTnT hearts maintained stroke volume. This observation implicates that the coexistence of eTnT might contribute a compensation for the impaired systolic function from the primarily pathogenic cTnT- $\Delta$ E7.

Nonetheless, the presence of an additional class of TnT in  $\Delta$ E7+eTnT double-transgenic mouse hearts increases myofilament heterogeneity that would decrease cardiac efficiency (Feng and Jin 2010). The in vivo cardiac function (Fig. 3A and B) showed that in contrast to that of cTnT- $\Delta$ E7 hearts,  $\Delta$ E7+eTnT hearts had diminished kinetic response to isoproterenol stimulation. The preload responses shown in Fig. 9 also indicated that  $\Delta$ E7+eTnT hearts had the lowest inotropic function at multiple levels of preloads. Therefore, the potential benefit of coexistence of embryonic cardiac TnT to compensate for the impaired function of cTnT- $\Delta$ E7 hearts is limited by the negative effect on reducing cardiac efficiency.

### Acknowledgments

We thank Dr. M.M. Hossain for maintaining the transgenic mouse lines and Hui Wang for mouse genotyping.

### Conflict of Interest

No competing financial interests are declared by the author(s).

### References

- Akella, A. B., X. L. Ding, R. Cheng, and J. Gulati. 1995. Diminished  $\text{Ca}^{2+}$  sensitivity of skinned cardiac muscle contractility coincident with troponin T-band shifts in the diabetic rat. *Circ. Res.* 76:600–606.
- Anderson, P. A., A. Greig, T. M. Mark, N. N. Malouf, A. E. Oakeley, R. M. Ungerleider, et al. 1995. Molecular basis of human cardiac troponin T isoforms expressed in the developing, adult, and failing heart. *Circ. Res.* 76:681–686.
- Barbato, J. C., Q. Q. Huang, M. M. Hossain, M. Bond, and J. P. Jin. 2005. Proteolytic N-terminal truncation of cardiac troponin I enhances ventricular diastolic function. *J. Biol. Chem.* 280:6602–6609.
- Biesiadecki, B. J., and J. P. Jin. 2002. Exon skipping in cardiac troponin T of turkeys with inherited dilated cardiomyopathy. *J. Biol. Chem.* 277:18459–18468.
- Biesiadecki, B. J., B. D. Elder, Z. B. Yu, and J. P. Jin. 2002. Cardiac troponin T variants produced by aberrant splicing of multiple exons in animals with high instances of dilated cardiomyopathy. *J. Biol. Chem.* 277:50275–50285.

- Biesiadecki, B. J., S. M. Chong, T. M. Nosek, and J. P. Jin. 2007. Troponin T core structure and the regulatory NH<sub>2</sub>-terminal variable region. *Biochemistry* 46:1368–1379.
- Braunwald, E., S. J. Sarnoff, and W. N. Stainsby. 1958. Determinants of duration and mean rate of ventricular ejection. *Circ. Res.* 6:319–325.
- Cooper, T. A., and C. P. Ordahl. 1985. A single cardiac troponin T gene generates embryonic and adult isoforms via developmentally regulated alternate splicing. *J. Biol. Chem.* 260:11140–11148.
- Feng, H. Z., and J. P. Jin. 2010. Coexistence of cardiac troponin T variants reduces heart efficiency. *Am. J. Physiol. Heart Circ. Physiol.* 299:H97–H105.
- Feng, H. Z., B. J. Biesiadecki, Z. B. Yu, M. M. Hossain, and J. P. Jin. 2008. Restricted N-terminal truncation of cardiac troponin T: a novel mechanism for functional adaptation to energetic crisis. *J. Physiol.* 586:3537–3550.
- Gauthier, N. S., G. P. Matherne, R. R. Morrison, and J. P. Headrick. 1998. Determination of function in the isolated working mouse heart: issues in experimental design. *J. Mol. Cell. Cardiol.* 30:453–461.
- Geraerts, T., P. Albaladejo, A. D. Declere, J. Duranteau, J. P. Sales, and D. Benhamou. 2004. Decrease in left ventricular ejection time on digital arterial waveform during simulated hypovolemia in normal humans. *J. Trauma* 56:845–849.
- Gomes, A. V., G. Venkatraman, J. P. Davis, S. B. Tikunova, P. Engel, R. J. Solaro, et al. 2004. Cardiac troponin T isoforms affect the Ca<sup>2+</sup> sensitivity of force development in the presence of slow skeletal troponin I: insights into the role of troponin T isoforms in the fetal heart. *J. Biol. Chem.* 279:49579–49587.
- Gordon, A. M., E. Homsher, and M. Regnier. 2000. Regulation of contraction in striated muscle. *Physiol. Rev.* 80:853–924.
- Gutterman, D. D., and A. W. Jr Cowley. 2006. Relating cardiac performance with oxygen consumption: historical observations continue to spawn scientific discovery. *Am. J. Physiol. Heart Circ. Physiol.* 291:H2555–H2556.
- Huang, Q. Q., F. V. Brozovich, and J. P. Jin. 1999. Fast skeletal muscle troponin T increases the cooperativity of transgenic mouse cardiac muscle contraction. *J. Physiol.* 520 (Pt 1):231–242.
- Huang, Q. Q., H. Z. Feng, J. Liu, J. Du, L. B. Stull, C. S. Moravec, et al. 2008. Co-expression of skeletal and cardiac troponin T decreases mouse cardiac function. *Am. J. Physiol. Cell Physiol.* 294:C213–C222.
- Jin, J. P. 1996. Alternative RNA splicing-generated cardiac troponin T isoform switching: a non-heart-restricted genetic programming synchronized in developing cardiac and skeletal muscles. *Biochem. Biophys. Res. Commun.* 225: 883–889.
- Jin, J. P., and S. M. Chong. 2010. Localization of the two tropomyosin-binding sites of troponin T. *Arch. Biochem. Biophys.* 500:144–150.
- Jin, J. P., and J. J. Lin. 1988. Rapid purification of mammalian cardiac troponin T and its isoform switching in rat hearts during development. *J. Biol. Chem.* 263:7309–7315.
- Jin, J. P., and J. J. Lin. 1989. Isolation and characterization of cDNA clones encoding embryonic and adult isoforms of rat cardiac troponin T. *J. Biol. Chem.* 264:14471–14477.
- Jin, J. P., and D. D. Root. 2000. Modulation of troponin T molecular conformation and flexibility by metal ion binding to the NH<sub>2</sub>-terminal variable region. *Biochemistry* 39:11702–11713.
- Jin, J. P., Q. Q. Huang, H. I. Yeh, and J. J. Lin. 1992. Complete nucleotide sequence and structural organization of rat cardiac troponin T gene. A single gene generates embryonic and adult isoforms via developmentally regulated alternative splicing. *J. Mol. Biol.* 227:1269–1276.
- Jin, J. P., J. Wang, and J. Zhang. 1996. Expression of cDNAs encoding mouse cardiac troponin T isoforms: characterization of a large sample of independent clones. *Gene* 168:217–221.
- Jin, J. P., A. Chen, O. Ogut, and Q. Q. Huang. 2000. Conformational modulation of slow skeletal muscle troponin T by an NH<sub>2</sub>-terminal metal-binding extension. *Am. J. Physiol. Cell Physiol.* 279:C1067–C1077.
- Jin, J. P., F. W. Yang, Z. B. Yu, C. I. Ruse, M. Bond, and A. Chen. 2001. The highly conserved COOH terminus of troponin I forms a Ca<sup>2+</sup>-modulated allosteric domain in the troponin complex. *Biochemistry* 40:2623–2631.
- Jin, J. P., Z. Zhang, and J. A. Bautista. 2008. Isoform diversity, regulation, and functional adaptation of troponin and calponin. *Crit. Rev. Eukaryot. Gene Expr.* 18:93–124.
- Lewis, R. P., S. E. Rittogers, W. F. Froester, and H. Boudoulas. 1977. A critical review of the systolic time intervals. *Circulation* 56:146–158.
- Li, Y., L. Zhang, P. Y. Jean-Charles, C. Nan, G. Chen, J. Tian, et al. 2013. Dose-dependent diastolic dysfunction and early death in a mouse model with cardiac troponin mutations. *J. Mol. Cell. Cardiol.* 62:227–236.
- Mamidi, R., S. L. Mallampalli, D. F. Wiczorek, and M. Chandra. 2013a. Identification of two new regions in the N-terminus of cardiac troponin T that have divergent effects on cardiac contractile function. *J. Physiol.* 591:1217–1234.
- Mamidi, R., J. J. Michael, M. Muthuchamy, and M. Chandra. 2013b. Interplay between the overlapping ends of tropomyosin and the N terminus of cardiac troponin T affects tropomyosin states on actin. *FASEB J.* 27:3848–3859.
- McConnell, B. K., C. S. Moravec, and M. Bond. 1998. Troponin I phosphorylation and myofilament calcium sensitivity during decompensated cardiac hypertrophy. *Am. J. Physiol.* 274:H385–H396.
- Mesnard-Rouiller, L., J. J. Mercadier, G. Butler-Browne, M. Heimbürger, D. Logeart, P. D. Allen, et al. 1997. Troponin T mRNA and protein isoforms in the human left ventricle: pattern of expression in failing and control hearts. *J. Mol. Cell. Cardiol.* 29:3043–3055.

- Neely, J. R., H. Liebermeister, E. J. Battersby, and H. E. Morgan. 1967. Effect of pressure development on oxygen consumption by isolated rat heart. *Am. J. Physiol.* 212:804–814.
- Ogut, O., H. Granzier, and J. P. Jin. 1999. Acidic and basic troponin T isoforms in mature fast-twitch skeletal muscle and effect on contractility. *Am. J. Physiol.* 276:C1162–C1170.
- Perry, S. V. 1998. Troponin T: genetics, properties and function. *J. Muscle Res. Cell Motil.* 19:575–602.
- Reiser, P. J., M. L. Greaser, and R. L. Moss. 1992. Developmental changes in troponin T isoform expression and tension production in chicken single skeletal muscle fibres. *J. Physiol.* 449:573–588.
- Reiser, P. J., M. L. Greaser, and R. L. Moss. 1996. Contractile properties and protein isoforms of single fibres from the chicken pectoralis red strip muscle. *J. Physiol.* 493(Pt 2):553–562.
- Sarnoff, S. J., E. Braunwald, G. H. Jr Welch, R. B. Case, W. N. Stainsby, and R. Macruz. 1958. Hemodynamic determinants of oxygen consumption of the heart with special reference to the tension-time index. *Am. J. Physiol.* 192:148–156.
- Wang, J., and J. P. Jin. 1997. Primary structure and developmental acidic to basic transition of 13 alternatively spliced mouse fast skeletal muscle troponin T isoforms. *Gene* 193:105–114.
- Wang, J., and J. P. Jin. 1998. Conformational modulation of troponin T by configuration of the NH<sub>2</sub>-terminal variable region and functional effects. *Biochemistry* 37:14519–14528.
- Wei, B., and J. P. Jin. 2011. Troponin T isoforms and posttranscriptional modifications: evolution, regulation and function. *Arch. Biochem. Biophys.* 505:144–154.
- Wei, B., J. Gao, X. P. Huang, and J. P. Jin. 2010. Mutual rescues between two dominant negative mutations in cardiac troponin I and cardiac troponin T. *J. Biol. Chem.* 285:27806–27816.
- Weissler, A. M., W. S. Harris, and C. D. Schoenfeld. 1968. Systolic time intervals in heart failure in man. *Circulation* 37:149–159.
- Yu, Z. B., H. Wei, and J. P. Jin. 2012. Chronic coexistence of two troponin T isoforms in adult transgenic mouse cardiomyocytes decreased contractile kinetics and caused dilatative remodeling. *Am. J. Physiol. Cell Physiol.* 303:C24–C32.
- Zhang, Z., B. J. Biesiadecki, and J. P. Jin. 2006. Selective deletion of the NH<sub>2</sub>-terminal variable region of cardiac troponin T in ischemia reperfusion by myofibril-associated mu-calpain cleavage. *Biochemistry* 45:11681–11694.